

Article

An Evaluation of the Variation in the Morphometric Parameters of Grain of Six *Triticum* Species with the Use of Digital Image Analysis

Klaudia Goriewa-Duba ¹, Adrian Duba ^{2,*}, Urszula Wachowska ² and Marian Wiwart ¹

¹ Department of Plant Breeding and Seed Production, University of Warmia and Mazury in Olsztyn, pl. Łódzki 3, 10-727 Olsztyn, Poland; klaudia.goriewa@uwm.edu.pl (K.G.-D.); wiwart@uwm.edu.pl (M.W.)

² Department of Entomology, Phytopathology and Molecular Diagnostics, University of Warmia and Mazury in Olsztyn, Prawocheńskiego 17, 10-719 Olsztyn, Poland; urszula.wachowska@uwm.edu.pl

* Correspondence: adrian.duba@uwm.edu.pl; Tel.: +48-523-35-97

Received: 28 September 2018; Accepted: 5 December 2018; Published: 7 December 2018



Abstract: Kernel images of six wheat species were subjected to shape and color analyses to determine variations in the morphometric parameters of grain. The values of kernel shape descriptors (area, perimeter, Feret diameter, minimal Feret diameter, circularity, aspect ratio, roundness, solidity) and color descriptors (H , S , I and $L^*a^*b^*$) were investigated. The influence of grain colonization by endophytic fungi on the color of the seed coat was also evaluated. Polish wheat grain was characterized by the highest intraspecific variation in shape and color. Bread wheat was most homogeneous in terms of the studied shape and color descriptors. An analysis of variations in wheat lines revealed greater differences in phenotypic traits of relict wheats, which have a larger gene pool. The grain of ancient wheat species was characterized by low roundness values and relatively low solidity. Shape and color descriptors were strongly discriminating components in the studied wheat species. Their discriminatory power was determined mainly by genotype. A method that supports rapid discrimination of cereal species and admixtures of other cereals in grain batches is required to guarantee the quality and safety of grain. The results of this study indicate that digital image analysis can be effectively used for this purpose.

Keywords: digital image analysis; wheat; multivariate analysis

1. Introduction

Hexaploid bread wheat (*Triticum aestivum* L. ssp. *aestivum*) grain is mostly processed into flour for baking and confectionery goods, and, to a smaller extent, into flour for the production of pasta and dumplings. The grain of tetraploid durum wheat (*T. turgidum* ssp. *durum* (Desf.) Husn.) is used mainly in the production of pasta and couscous [1]. The growing interest in healthy foods has contributed to the revival of ancient wheats. One of them is einkorn (*T. monococcum* L. ssp. *monococcum*), a diploid species that is abundant in protein, unsaturated fatty acids, lutein, and essential minerals, mainly zinc and iron [2]. The popularity of other tetraploid wheats: emmer (*T. turgidum* L. ssp. *dicoccum* (Schrank ex Schübl.) Thell.) and Polish wheat (*T. turgidum* L. ssp. *polonicum* (L.) Thell.) and hexaploid spelt (*T. aestivum* L. ssp. *spelta* (L.) Thell.), is also on the rise. The renewed interest in relict wheat species can be attributed to the fact that their grain is considered to be a functional food.

Long-term selection of bread and durum wheat, combined with genetic drift (random fluctuations in the number of gene alleles in a population) and the bottleneck effect (reduced population size due to sudden environmental events) have contributed to a considerable loss of genetic variation in these species [3,4]. On the other hand, relict wheats are characterized by a rich gene pool [5,6] which improves pathogen resistance. Fungal pathogens that synthesize mycotoxins that contaminate food products

pose the greatest threat for human and animal health. *Alternaria alternata* (Fr.) Keiss. and selected *Fusarium* species are the most ubiquitous toxin-producing pathogens of wheat grain. These fungi produce various pigments that can affect the color of the grain pericarp and the embryo [7,8]. The presence of these pathogens could be easily detected on the surface of wheat grain by digital image analysis.

The grain of *Triticum* species other than bread wheat requires complex processing technologies, and it is used in the production of various foods [9–11], which is why it should not come into contact with bread wheat grain during market operations. A reliable analysis of the morphometric parameters of grain can facilitate the development of effective tools for rapid and non-invasive quality control of consumer grain and seed material. The laws of the European Union [12], introduce increasingly stringent microbiological quality standards for foods, which has spurred the search for rapid, accurate and low-cost systems for monitoring plant materials during processing [13,14]. The EyeFoss™ (FOSS Analytical, Höganäs, Sweden) image analyzer is one of such systems. The device has been implemented in the food processing sector to eliminate subjectivity from quality assessments of sprouted wheat grain, weed seeds, unmillable material, and grain defects (insect damage, mold or germ damage) [15]. Traditional grain sorting and evaluation methods rely on sensory analyses, they are laborious and time-consuming, and the results are always burdened with a certain degree of error [16]. Digital image analysis can considerably facilitate these processes, and it has presently been used for plant phenotyping [17]. The first studies examining this analytical technique were conducted to verify the varietal identity of wheat kernels based on their shape and color descriptors [18,19] and to identify non-wheat components separated from wheat grain samples [20]. In the following years, digital image analysis was successfully used to evaluate the damage caused by insects on the surface of wheat grain [21] and to assess the health of maize grain [22]. Image analysis is also applied to assess the severity of fungal infections of leaves [23,24]. However, wheat grain infections have been rarely studied by digital image analysis [25,26]. Ahmad et al. [27] relied on image processing to discriminate healthy, diseased, and immature fruit seeds and cereal grain. The color of soybean seeds was described with 88% accuracy. Recently, Leplat et al. [28] successfully used computer-assisted image analysis to evaluate FHB (Fusarium Head Blight) symptoms on the surface of wheat grain. This approach could decrease the demand for expensive chromatographic analyses of the most prevalent mycotoxin, deoxynivalenol (DON), because it supports analyses of wheat grain already at the soft dough stage [28]. Research has also demonstrated that digital image analysis is a useful technique for discriminating the grain of different bread wheat varieties [29], bread wheat, and spelt hybrids and their parental forms [30], and the seeds of red clover varieties [31]. Ropelewska et al. [32] relied on digital image analysis to discriminate rapeseed varieties, and Chaugule and Mali [33]—to confirm the identity of rice varieties. Seed shape can be estimated on the basis of shape descriptors, diverse indexes, or by comparison with geometric figures (*J* index) where the description of the seed shape is based on percentage of similarity to a certain object. To get a more detailed review, see Cervantes et al. [34].

Digital image analysis software allows users to analyze hundreds of digital images per hour with a high degree of automation. Digital images are processed to eliminate defects such as: (1) geometric distortion, (2) poor contrast, (3) image noise, (4) uneven illumination. The analysis is preceded by image segmentation, during which regions of interest (ROI) are separated from the background [35]. The segmentation involves filtering and thresholding procedures [36,37]. Large datasets relating to the shape and color of the analyzed objects should be minimized [36].

In the images captured with a digital camera, color is represented by three primary colors: red, green, and blue, which are combined on the screen. Each sensor records a specific single color. The real color of an individual pixel is acquired with the use of an interpolation algorithm, which compares a pixel with the color information that is extracted from the neighboring pixels to estimate its actual color. The interpolation algorithm relies on the red, green and blue (RGB) model to depict the original color. The color of a pixel is described by hue, saturation, and intensity (HSI), where hue denotes the “pure” pixel color, saturation indicates the amount of color, and intensity

describes a pixel's brightness [38]. Variations in light and color have to be avoided during image analysis, especially in experiments where measurements have to be automated. Moreover, low saturation and intensity can disrupt the segmentation process [39]. Resolution and image compression also influence image quality [40]. Image resolution affects data storage space, and the acquired images are large files. File size and resolution can be reduced, but this could affect the quality of the image [38].

The aim of this study was to discriminate six *Triticum* taxa based on the shape and color descriptors of kernel images. The grain was also analyzed to determine whether the presence of pathogenic fungi can influence the color of kernels. The results were processed by principal component analysis (PCA) and hierarchical clustering. The presence of fungal pathogens on wheat grain can be evaluated by image processing based on grain color, which supports a quick assessment of grain quality. Image analysis is a highly promising tool for evaluating the health status of wheat grain and forecasting the results of decision support tools. To the best of the authors' knowledge, there are no comprehensive studies which rely on the above approach to detect multiple biotic stressors in wheat grain. The growing demand for healthy wheat-based foods of high quality should encourage food producers to use effective and inexpensive methods in the process of screening for the best raw materials.

2. Materials and Methods

The experimental material comprised the grain of six spring wheat taxa: bread wheat (*T. aestivum* ssp. *aestivum*, *Taa*, two lines), spelt (*T. aestivum* L. ssp. *spelta*, *Tas*, nine lines), durum wheat (*T. turgidum* ssp. *durum*, *Ttdu*, three lines), Polish wheat (*T. turgidum* L. ssp. *polonicum*, *Ttp*, 17 lines), emmer (*T. turgidum* ssp. *dicoccum*, *Ttdi*, 23 lines) and einkorn (*T. monococcum* ssp. *monococcum*, *Tmm*, three lines). All lines were reproduced at the Department of Plant Breeding and Seed Production of the University of Warmia and Mazury in Olsztyn, Poland. The lines were obtained by the reproduction of accessions obtained from National Centre for Plant Genetic Resources (NCPGR), Radzików, Poland, National Plant Germplasm System (NPGS), USA, Leibniz Institute of Plant Genetics and Crop Plant Research (IPK) in Gatersleben, Germany. A field experiment was conducted in 2014/2015 in the Agricultural Experiment Station in Bałcyny (53°36' N, 19°51' E), Poland. Plots with an area of 9 m² each were established on soil typically used for wheat cultivation. The preceding crop was a mixture of cereals and legumes. Before sowing, plots were fertilized with 20/70/95 kg N/P₂O₅/K₂O ha⁻¹. The second rate of the N fertilizer was applied in May at 20 kg ha⁻¹. All wheats were sown at a rate of 400 germinating kernels per m². The grains of wheat species were subjected to shape and color analysis, and then analyzed for fungal presence.

2.1. Image Analysis

Digital images were acquired with a flatbed CCD scanner (Epson Perfection V370 Photo, Epson, Shinjuku, Tokyo, Japan) with a true optical resolution of 4800 dpi, connected to a PC with Windows 10. The image analysis was performed with the ImageJ program (v. 1.51h, Laboratory for Optical and Computational Instrumentation, Madison, WI, USA) [41]. All measurements were carried out in three replications. Each replication consisted of 50 selected randomly kernels, placed on the scanner screen with the crease down. A dark paper background (located above the flatbed scanner) with the predominance of the blue component ($R = 100, G = 140, B = 200$) was used to increase contrast between the kernel images and the background. Color images at 24-bit with 200 dpi resolution were recorded in BMP (Bitmap Image File) format. At the beginning of image segmentation, a median filter was applied to reduce noise (radius of four pixels, one replication). The color thresholding procedure was performed in an identical manner for all analyzed images, and a lower threshold value was set for the color component R at 120. This procedure thresholds 24-bit RGB images based on hue, saturation, and intensity (HSI), red, green and blue (RGB), $CIE L^*a^*b^*$ (expresses color as three numerical values, L^* for the lightness and a^* and b^* for the green–red and blue–yellow color components), or YUV

(Y is a luminance component while U and V are chrominance components). Filter ranges can be set manually, or based on the pixel value components of a user-defined region of interest (experimental). A thresholded image is an RGB image, not an 8-bit grayscale image. Color images were copied to a new window with uniform black background. The above procedure was performed to generate images for shape and color analyses.

2.2. Shape Analysis

Shape analyses were performed on R-filtered images with the highest contrast between the kernel and the background (Figure 1). The following descriptors represented by blobs (ROI) were determined in images of individual kernels images: (1) area (mm^2), (2) perimeter (PE) (mm), (3) circularity (CI), (4) Feret diameter (FD), (5) minimal Feret diameter (MFD), (6) aspect ratio (AR), (7) roundness (RO), and (8) solidity (SO) (Table 1).

Table 1. The characteristics of the main shape and color descriptors.

Descriptor	Characteristics	Equation
Shape		
Area	The quantity that expresses the extent of a two-dimensional figure or shape	<i>n/a</i>
Perimeter (PE)	A path that surrounds a two-dimensional shape	<i>n/a</i>
Circularity (CI)	Shape factor, takes on values in a range from 0 (elongated shape) to 1 (perfect circle)	$Circ.=4\pi \times \frac{Area}{Perimeter^2}$
Feret Diameter (FD)	The longest distance between any two pixels along the selection boundary	<i>n/a</i>
Minimal Feret diameter (MFD)	The shortest distance between any two pixels along the selection boundary	<i>n/a</i>
Aspect ratio (AR)	Aspect ratio of the blob's fitted ellipse. Major and minor axis refer to the ellipse fitted to region of interest (ROI)	$AR=\frac{Major\ Axis}{Minor\ Axis}$
Roundness (RO)	Describes shapes conversely to AR	$Round.=\frac{Area}{(\pi \times (MajorAxis)^2)}$
Solidity (SO)	Describes ROI with regard to shape regularity. The Convex Area refers to the area of the convex hull of the region (the smallest region that is convex and that contains the original ROI). The value of this descriptor is lower for objects with an irregular shape, and higher for objects with a regular shape	$Solid.=\frac{Area}{Convex\ Area}$
Color		
Hue (H)	Refers to the attribute of visible light due to that is differentiated from or similar to red, green or blue	<i>Formulas proposed by Wiewart et al. [42]</i>
Saturation (S)	Proportion of pure chromatic color in the total color sensation	
Intensity (I)	Refers to the amount of light or the numerical value of a pixel	
Luminance (L^*)	Measures perceived "gray-level" of pixel	
a^*	Denotes redness–greenness	
b^*	Denotes yellowness–blueness	



Figure 1. Typical kernel images of the analyzed wheat species. **A**—einkorn, **B**—emmer, **C**—durum wheat, **D**—Polish wheat, **E**—bread wheat, **F**—spelt.

2.3. Color Analysis

The 24-bit color images were converted to three 8-bit images in channels R , G , B . The color analysis was conducted based on the average values of variables R , G , B for every ROI, which were later used to calculate the values of H , S , I and $L^*a^*b^*$. Parameter H denotes hue, S denotes saturation, I denotes intensity, L^* denotes luminance (100 = white and 0 = black), a^* denotes redness–greenness, and b^* denotes yellowness–blueness. The variables R , G , B were converted to H , S , I and to $L^*a^*b^*$ according to the formulas proposed by Wiwart et al. [42]. Color measurements were expressed with parameters H , S , I and $L^*a^*b^*$.

2.4. Fungal Colonization of Grain

Wheat heads from the field experiment were harvested manually at maturity and threshed. Randomly selected kernels were subjected to image analysis, and 25 kernels from each wheat line were used to determine the prevalence of fungal pathogens in spring wheat grain. Kernels were surface-disinfected in 1% NaOCl (for endophyte counts) for 1 min and placed on potato dextrose agar (PDA, Merck, Warsaw, Poland), pH = 5.5 [43]. Five kernels from every wheat line were placed on a Petri plate in five replications. The above procedure was performed under sterile conditions. Fungi were transferred to PDA slants and identified based on mycological keys [44,45]. Fungi were identified based on a morphological description of spores and mycelia, colony appearance, color, and shape. The number of endophytic fungal colonies was counted after seven days of incubation at 24 °C. Fungal filaments characteristic of the genus *Fusarium* were isolated and transferred to individual Petri plates to determine their identity under a light microscope (Nikon Eclipse, Tokyo, Japan). Specimens of fungal filaments were viewed under 400× magnification. Fungal pathogens colonizing the grain of the evaluated wheats were identified to species level to verify the hypothesis that fungal infections can influence grain color.

2.5. Statistical Analysis

The results of image analysis were processed statistically using STATISTICA 12 software (StatSoft Polska, Cracow, Poland) [46]. The significance of differences between mean values was estimated by analysis of variance, and the mean values were compared by Tukey’s test. The morphological traits of kernels (shape and color) were analyzed by agglomerative hierarchical clustering (Ward method with the application of Euclidean distances) using STATISTICA 12 software [46]. The cluster analysis was performed on eight and six shape and color parameters of 50 wheat lines classified into six wheat species. Shape and color descriptors were also processed by PCA. The results of PCA were presented in graphic form. A correlation analysis was carried out for all compared shape and color descriptors and for single kernel weight.

3. Results

The analyzed *Triticum* species differed significantly in single kernel weight (Table 2), which was significantly highest in durum wheat (61.00 mg) and lowest in einkorn (27.29 mg). The grain of the evaluated wheat species also differed significantly in shape and color descriptors.

Table 2. Average single kernel weight (SKW) of the investigated wheat species.

SKW (mg)					
<i>Taa</i>	<i>Tas</i>	<i>Ttdu</i>	<i>Ttp</i>	<i>Ttdi</i>	<i>Tmm</i>
42.13 ^{bc}	49.69 ^b	61.00 ^a	46.92 ^b	39.84 ^c	27.29 ^d

a, b, c, d—mean values marked with the same letter do not differ significantly in Tukey's test at $p \leq 0.01$.

Taa—*T. aestivum* ssp. *aestivum*, *Tas*—*T. aestivum* ssp. *spelta*, *Ttdu*—*T. turgidum* ssp. *durum*, *Ttp*—*T. turgidum* ssp. *polanicum*, *Ttdi*—*T. turgidum* ssp. *dicoccum*, *Tmm*—*T. monococcum* ssp. *monococcum*.

3.1. Shape Analysis

A typical image of kernel surface in all analyzed wheat species is presented in Figure 1. Kernel image area was characterized by the highest intraspecific variation. The relative standard deviation (RSD) for this trait ranged from 3% in einkorn to more than 15% in Polish wheat. SO was the least varied trait, and its RSD was below 1% in all species (Table 3). The images of Polish wheat kernels revealed the highest intraspecific variation in PE, FD, SO, AR, and RO (Table 3). The lowest intraspecific variations were observed in bread wheat grain, which was most homogeneous in terms of CI, MFD, AR, RO, and SO. Durum wheat grain was also relatively homogeneous in terms of area, PE, and FD (Table 3).

An analysis of interspecific variations revealed that images of einkorn kernels were characterized by the smallest area and a narrow shape, as exemplified by the lowest values of Area (8.7–20.1 mm²) and MFD (1.9–3.4 mm), and the highest AR values (2.3–3.9) in comparison with other taxa (Table 3). Einkorn kernels were also the most elongated (low value of RO at 0.3–0.4) and had the least regular shape (SO = 0.8–1.0). The images of emmer kernels were characterized by a large perimeter (PE = 12.0–41.8), and a high value of FD and low value of CI. Emmer kernels images were only bigger than einkorn and bread wheat grain; however, their shape was more elongated. The highest average area was noted in the grains of Polish wheat, durum wheat and spelt, and these findings were confirmed by cluster analysis (Figure 2). In Polish wheat and spelt, large grain area was correlated with high perimeter values (PE = 13.7–32.6 and 14.3–31.2, respectively) (Table 3; Figure 2). The grain of the above wheat species was also characterized by an elongated shape, and CI values ranged from 0.3 to 0.8 in Polish wheat. Spelt kernels were also considerably elongated (FD = 5.4–10.5, CI = 0.4–0.8) and wide (MFD = 2.2–4.6), and similar observations were made in durum wheat (Table 3; Figure 2). The images of bread and durum wheat grain was characterized by more regular structures (SO = 0.963 and 0.980, respectively) than ancient wheats grain (i.e., einkorn SO value at 0.947 or emmer at 0.950). Images of durum kernels were more elongated (lower values of RO and higher values of AR and FD) than bread wheat grain.

In the cluster analysis of shape descriptors, the evaluated wheat lines were grouped into two major clusters (Figure 2). The first major cluster consisted of bread wheat, durum wheat, spelt, and Polish wheat lines which were further subdivided into four minor clusters (*a–d*). The minor cluster *a* was composed exclusively of bread wheat lines whose grain was generally characterized by average or low values of most descriptors. The only exceptions were high values of CI, MFD, and RO, which are indicative of oval-shaped kernels, and high values of SO, which point to regularly shaped kernels. The minor cluster *b* comprised various lines of tetraploid wheat, including durum wheat, Polish wheat, and emmer, as well as two lines of hexaploid spelt. Most wheat lines grouped in the minor clusters *b* differed from the minor cluster *a* in terms of grain size. The grain of most lines in the minor cluster *b* was larger than bread wheat grain. The minor cluster *c* was composed of spelt lines, which formed internal nodes with lines of Polish wheat and emmer. These lines were characterized by large, irregular, and elongated kernels. The minor cluster *d* contained mostly Polish wheat lines, which were grouped in internal nodes, as well as two spelt lines, which formed a separate internal node. Their grain was significantly more elongated and irregular than the grain of wheat lines in the minor cluster *c* (Figure 2).

Table 3. The values of shape descriptors taken into consideration in the kernel image analysis of wheat species.

MV	Taa	Tas	Ttdu	Ttp	Ttdi	Tmm	Taa	Tas	Ttdu	Ttp	Ttdi	Tmm	Taa	Tas	Ttdu	Ttp	Ttdi	Tmm
	Area (mm ²)						PE (mm)						CI					
Mean	15.24 ^{bc}	20.54 ^a	19.55 ^a	19.68 ^a	17.26 ^b	12.89 ^c	15.80 ^c	20.06 ^a	18.81 ^{ab}	19.93 ^a	19.26 ^a	17.52 ^{bc}	0.76 ^a	0.64 ^c	0.69 ^b	0.62 ^c	0.58 ^d	0.53 ^e
SD	0.77	2.02	0.93	3.04	1.56	0.39	0.37	1.22	0.36	1.77	0.90	0.38	0.01	0.02	0.01	0.03	0.04	0.02
RSD (%)	5.04	9.84	4.75	15.42	9.07	3.06	2.37	6.10	1.91	8.89	4.66	2.15	0.83	4.15	1.92	4.86	6.64	4.23
Min	7.58	11.42	9.50	9.22	7.74	8.73	11.73	14.30	14.28	13.65	11.97	14.06	0.56	0.36	0.49	0.34	0.32	0.24
Max	20.29	31.10	26.80	35.50	50.67	20.07	18.34	31.20	22.18	32.63	41.74	27.62	0.82	0.80	0.76	0.76	1.00	0.66
	FD (mm)						MFD (mm)						AR					
Mean	6.12 ^d	8.37 ^a	7.66 ^{bc}	8.26 ^{ab}	8.27 ^a	7.6 ^c	3.24 ^{ab}	3.35 ^a	3.32 ^{ab}	3.16 ^b	2.89 ^c	2.43 ^d	1.88 ^e	2.42 ^d	2.35 ^d	2.62 ^c	2.86 ^b	3.16 ^a
SD	0.14	0.54	0.13	0.83	0.48	0.20	0.08	0.14	0.09	0.16	0.23	0.07	0.02	0.13	0.05	0.23	0.26	0.14
RSD (%)	2.34	6.50	1.67	10.00	5.85	2.61	2.39	4.11	2.71	5.08	7.81	2.78	1.07	5.43	2.30	8.74	9.22	4.52
Min	4.76	5.35	5.95	5.65	4.64	5.92	1.89	2.17	1.87	1.90	1.69	1.89	1.41	1.73	1.91	1.05	1.43	2.26
Max	7.25	10.51	8.84	12.71	11.18	9.18	4.22	4.58	4.33	6.71	8.16	3.42	3.19	3.46	4.04	5.24	4.84	3.93
	RO						SO											
Mean	0.54 ^a	0.41 ^b	0.43 ^b	0.39 ^c	0.36 ^d	0.32 ^e	0.963 ^{ab}	0.958 ^{bc}	0.970 ^a	0.959 ^b	0.950 ^c	0.947 ^d						
SD	0.01	0.02	0.01	0.03	0.04	0.02	<0.01	<0.01	<0.01	0.01	0.01	0.01						
RSD (%)	1.04	5.78	1.97	8.34	10.28	4.88	0.21	0.30	0.37	0.55	0.53	0.43						
Min	0.31	0.29	0.25	0.19	0.21	0.25	0.92	0.88	0.92	0.75	0.80	0.82						
Max	0.71	0.58	0.52	0.96	1.00	0.44	0.97	0.97	0.98	0.98	1.00	0.96						

MV—measures of variation, PE—perimeter, CI—circularity, FD—Feret diameter, MFD—minimal Feret diameter, AR—aspect ratio, RO—roundness, SO—solidity. Taa—*T. aestivum* ssp. *aestivum*, Tas—*T. aestivum* ssp. *spelta*, Ttdu—*T. turgidum* ssp. *durum*, Ttp—*T. turgidum* ssp. *polonicum*, Ttdi—*T. turgidum* ssp. *dicoccum*, Tmm—*T. monococcum* ssp. *monococcum*. a, b, c, d, e—mean values marked with the same letter do not differ significantly in Tukey's test at $p \leq 0.01$.

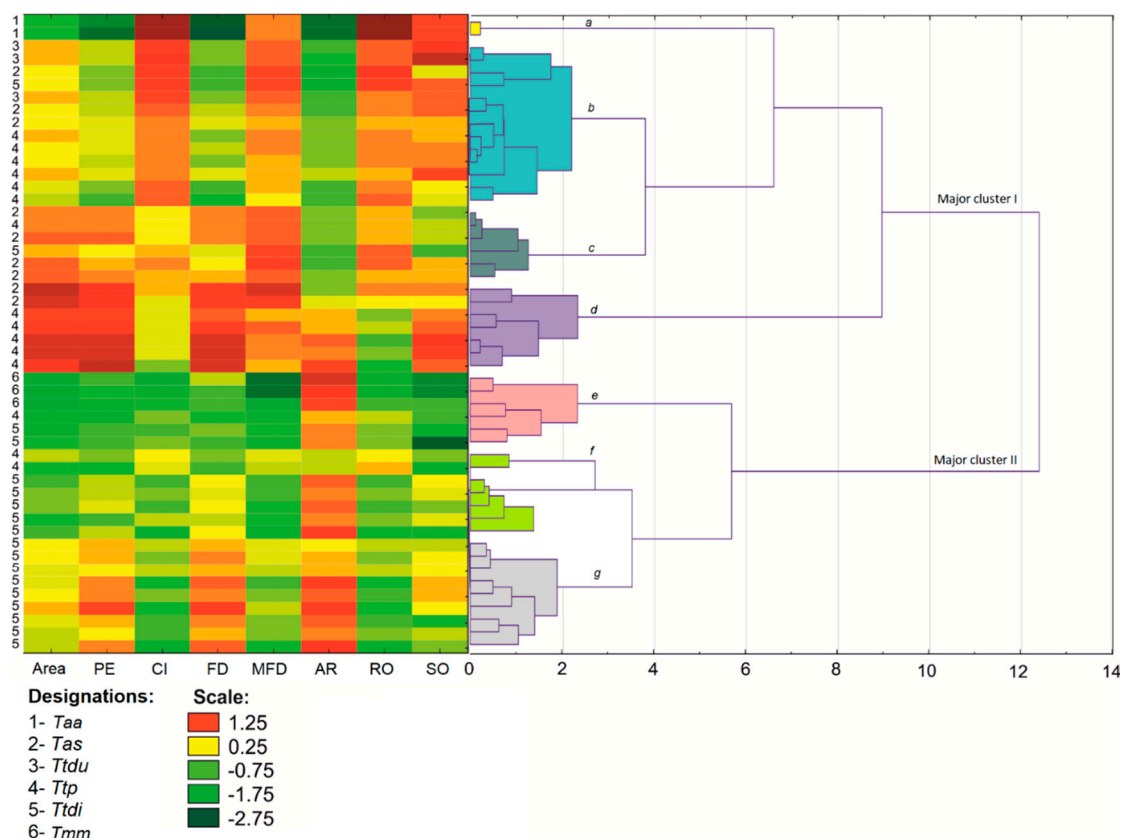


Figure 2. A heat map and the results of cluster analysis of kernel shape descriptors in the analyzed wheat species. PE—perimeter, CI—circularity, FD—Feret diameter, MFD—minimal Feret diameter, AR—aspect ratio, RO—roundness, SO—solidity, *Taa*—*T. aestivum* ssp. *aestivum*, *Tas*—*T. aestivum* ssp. *spelta*, *Ttdu*—*T. turgidum* ssp. *durum*, *Ttp*—*T. turgidum* ssp. *polonicum*, *Ttdi*—*T. turgidum* ssp. *dicoccum*, *Tmm*—*T. monococcum* ssp. *monococcum*, *a, b, c, d, e, f, g*—minor cluster name.

The second major cluster was subdivided into three minor clusters (*e–g*). The minor cluster *e* contained einkorn lines, one Polish wheat line, and two emmer lines. Their grain was characterized by a relatively small image area and low values of CI. The minor cluster *f* grouped two lines of Polish wheat which formed a strong internal node as well as several emmer lines. These lines differed only in AR and RO, and the remaining descriptors were similar in both species. The minor cluster *g* comprised only emmer lines whose grain was larger (area) and more regularly shaped (SO) in comparison with the emmer lines grouped in the minor cluster *f* (Figure 2).

The cluster analysis revealed significant intraspecific variations in Polish wheat, where shape descriptors ranged across a wide range of values. Bread wheat and durum wheat lines were characterized by low levels of variation in the above parameter (Figure 2).

3.2. Color Analysis

The color analysis also revealed noticeable variations between the analyzed wheat species (Table 4). Similarly to the shape analysis, Polish wheat kernels were characterized by the greatest variations in color, and considerable differences in color components *H*, *S*, *L** and *a** (RSD of 5%, 15.1%, 0.6% and 14.9%, respectively) were observed. Color components were least varied in spelt kernels (Table 4). In all analyzed wheat species, the greatest variations were noted in parameter *b** where RSD values ranged from 10.9% in durum wheat to 17.5% in bread wheat.

Similarly to the shape analysis, the hierarchical clustering supported the classification of wheat lines into two major clusters (Figure 3). The first major cluster was subdivided into five minor clusters (*a–e*). The minor cluster *a* was composed of one bread wheat line and four Polish wheat lines whose

kernels were characterized by low values of color intensity (I) and average and low values of luminance (L^*). The above results are indicative of darker grain. The minor cluster b contained one line of bread wheat, Polish wheat, and spelt each, and two emmer lines. These lines were characterized by generally higher values of I and L^* in comparison with the previous cluster. The minor cluster c was composed of only Polish wheat lines characterized by very light kernels with a yellow–green hue (H). The minor clusters d comprised only durum wheat lines with very high values of H , S and L^* . The last minor cluster e grouped einkorn and Polish wheat lines with similarly colored kernels that differed only in the lower values of color descriptor b^* (Figure 3).

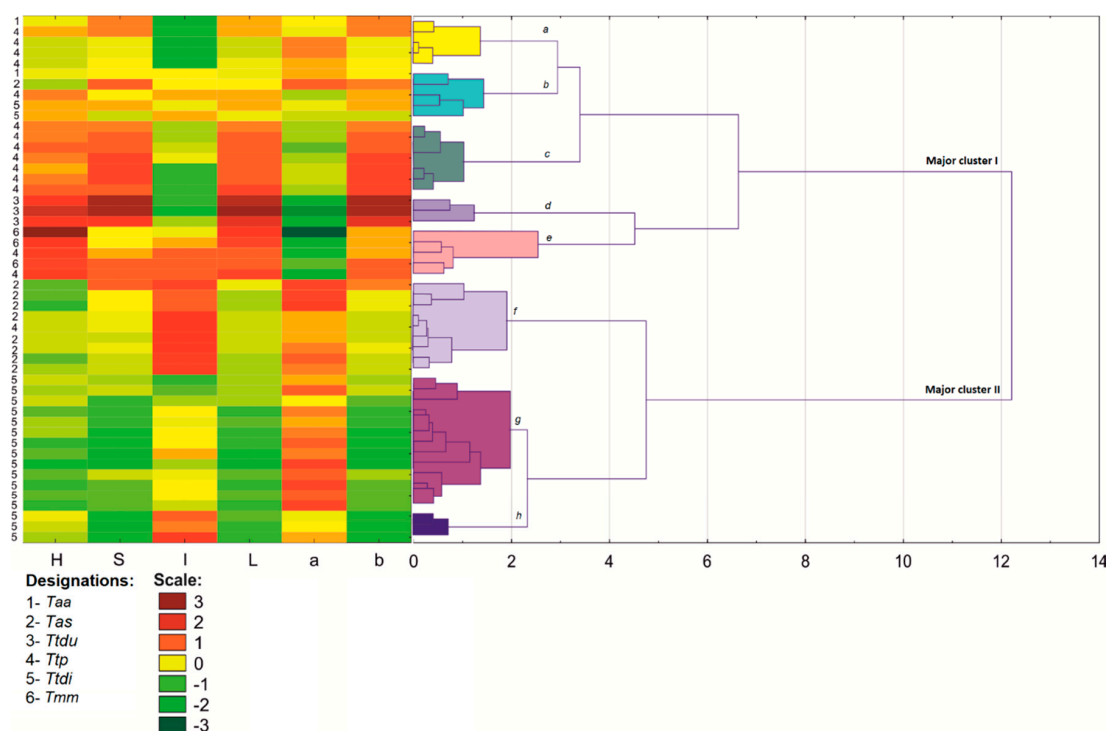


Figure 3. A heat map and the results of cluster analysis of kernel color descriptors in the analyzed wheat species. H —hue, S —saturation, I —intensity, L^* —luminance, a^* indicates redness–greenness and b^* indicates yellowness–blueness, *Taa*—*T. aestivum* ssp. *aestivum*, *Tas*—*T. aestivum* ssp. *spelta*, *Ttdu*—*T. turgidum* ssp. *durum*, *Ttp*—*T. turgidum* ssp. *polonicum*, *Ttdi*—*T. turgidum* ssp. *dicoccum* *Tmm*—*T. monococcum* ssp. *monococcum*, a , b , c , d , e , f , g , h —minor cluster name.

The second major cluster was subdivided into three minor clusters (f – h). The minor cluster f was composed of spelt lines with low values of H . The minor cluster g grouped emmer lines whose kernels were characterized by lower color intensities in comparison with spelt. The minor cluster h also comprised emmer lines whose color intensity was similar to that of spelt (Figure 3).

Table 4. The values of color descriptors taken into consideration in kernel image analysis of wheat species.

MV	Taa	Tas	Ttdu	Ttp	Ttdi	Tmm	Taa	Tas	Ttdu	Ttp	Ttdi	Tmm	Taa	Tas	Ttdu	Ttp	Ttdi	Tmm	
			H						S						I				
Mean	35.37 ^{bc}	33.94 ^c	40.36 ^a	36.79 ^b	34.05 ^c	40.71 ^a	0.21 ^{bc}	0.20 ^c	0.25 ^a	0.21 ^b	0.18 ^d	0.21 ^{bc}	0.48 ^{cd}	0.52 ^a	0.47 ^d	0.48 ^c	0.50 ^b	0.50 ^b	
SD	1.09	0.96	1.70	1.86	1.11	1.85	0.02	0.01	0.02	0.04	0.01	0.02	0.03	0.02	0.02	0.03	0.02	0.02	
RSD (%)	3.08	2.82	4.21	5.00	3.26	4.56	10.82	6.97	7.06	15.09	7.79	8.89	5.81	3.98	4.88	5.47	4.09	4.05	
Min	29.29	28.96	33.58	13.29	5.53	34.87	0.13	0.13	0.19	0.13	0.07	0.15	0.40	0.42	0.38	0.36	0.39	0.43	
Max	38.28	88.76	52.73	64.93	118.6	50.32	0.27	0.27	0.33	0.30	0.28	0.27	0.59	0.61	0.54	0.62	0.62	0.58	
			L*						a*						b*				
Mean	65.50 ^{cd}	65.39 ^d	65.99 ^a	65.59 ^c	65.3 ^e	65.75 ^b	−4.82 ^{ab}	−4.52 ^a	−6.03 ^c	−5.16 ^b	−4.69 ^a	−6.04 ^c	6.96 ^{bc}	6.38 ^c	9.51 ^a	7.19 ^b	5.26 ^d	7.20 ^b	
SD	0.11	0.08	0.15	0.39	0.08	0.12	0.32	0.25	0.45	0.71	0.25	0.39	1.22	0.75	1.04	0.91	0.75	1.02	
RSD (%)	0.17	0.12	0.23	0.60	0.12	0.19	6.55	5.56	7.47	14.94	5.38	6.53	17.49	11.72	10.9	13.68	14.34	14.21	
Min	65.10	65.13	65.51	61.2	61.58	65.32	−5.59	−12.18	−8.73	−12.00	−10.26	−7.82	2.80	3.74	6.03	−9.42	−16.36	3.91	
Max	65.85	66.53	66.58	67.25	66.74	66.16	−3.17	−3.10	−4.25	9.06	2.34	−4.55	9.96	10.20	14.11	11.66	10.61	10.18	

MV— measures of variation, H—hue, S—saturation, I—intensity, L*—luminance, a* indicates redness–greenness and b* indicates yellowness–blueness. Taa—*T. aestivum* ssp. *aestivum*, Tas—*T. aestivum* ssp. *spelta*, Ttdu—*T. turgidum* ssp. *durum*, Ttp—*T. turgidum* ssp. *polonicum*, Ttdi—*T. turgidum* ssp. *dicoccum*, Tmm—*T. monococcum* ssp. *monococcum*. a, b, c, d, e—mean values marked with the same letter do not differ significantly in Tukey's test at $p \leq 0.01$.

3.3. Correlation Analysis

The correlation analysis revealed statistically significant, but not strong interrelationships between most shape and color descriptors. Highly significant correlations ($p < 0.01$) were noted between PE vs Area ($r = 0.862$) and FD ($r = 0.96$), between CI and RO ($r = 0.959$), between L^* vs. H ($r = 0.920$) and b^* ($r = 0.944$), and between S and b^* ($r = 0.995$) (Table 5). These results indicate that PE and FD increased with kernel area. Strong negative correlations were observed between AR and CI ($r = -0.958$), AR and RO ($r = -0.985$), and between a^* and H ($r = -0.989$) and L^* ($r = -0.879$) (Table 5). Variables L^* and S were positively correlated with b^* , which implies that the contribution of yellowness increased with lightness and saturation. A strong linear correlation ($p < 0.01$) was also noted between SKW vs Area ($r = 0.537$) and MFD ($r = 0.583$) (Table 5), which suggests that regularly shaped and largest kernels were heaviest. Interestingly, SKW was positively correlated with MFD, but not FD, which indicates that wider kernels are heavier, whereas kernel length does not significantly influence weight.

3.4. Identification of Fungi

A mycological analysis revealed that the grain of all analyzed wheat species was most abundantly colonized by *A. alternata* (Figure 4), which accounted for 78% of all pathogenic fungi isolated from bread wheat and for more than 99% of all pathogenic fungi isolated from einkorn and spelt. Kernels were also colonized by fungi of the genera *Fusarium* (*Fusarium poae* (Peck) Wollenw and *Fusarium sporotrichioides* Sherbakoff), *Epicoccum nigrum* Link, *Drechslera* sp., and *Penicillium* sp. (Figure 4). Other fungal species were present in trace amounts on einkorn, Polish wheat, durum wheat, and spelt kernels, whereas *Fusarium* fungi, *F. poae*, and *F. sporotrichioides* accounted for nearly 10% of pathogens isolated from emmer. Bread wheat was noticeably colonized by *F. poae*, which was identified in 16% of isolates (Figure 4). *A. alternata* colonies were generally dark brown to dark olive-green in color, and they produced characteristic long chains of oval to ellipsoid conidia. *Fusarium poae* produced orange–pink mycelia with spherical conidia in conidiophores, whereas *F. sporotrichioides* was identified based on the presence of numerous oval microconidia with short terminal tips. *Epicoccum nigrum* was identified based on the presence of round, multiseptate conidia, and *Drechslera* sp.—based on the presence of ellipsoid and somewhat elongated conidia. *Penicillium* sp. were detected based on the morphological traits of spores in chains and green–white mycelia. However, there were no significant correlations between fungal colonization and the color of the seed coat.

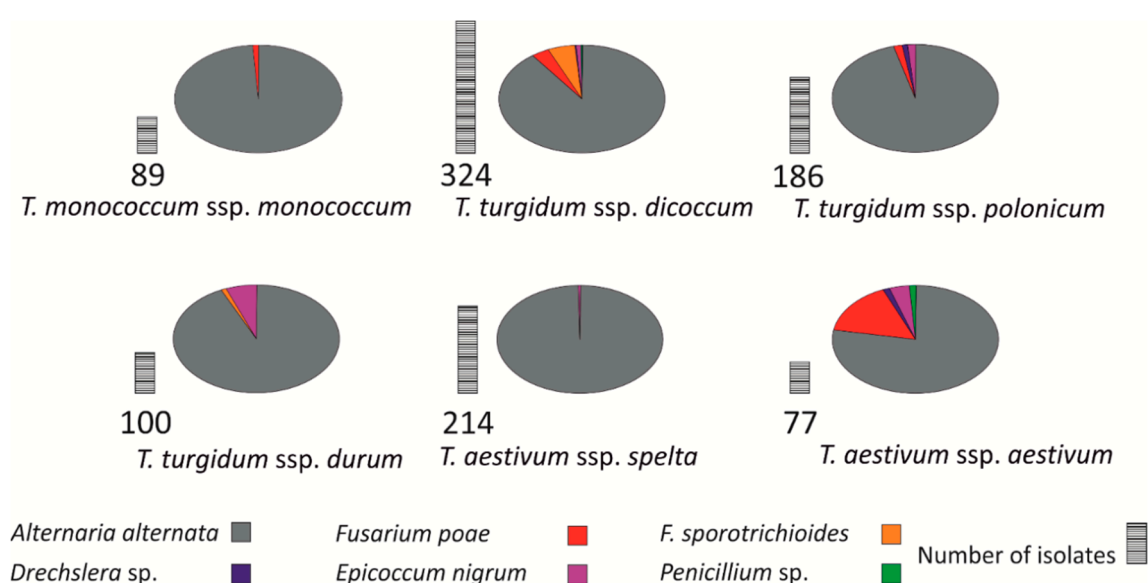


Figure 4. Colonization of wheat grain by endophytic fungi. The vertical bars represent the counts of fungal colonies in wheat grain.

Table 5. Pearson's correlation coefficient matrix for all investigated image shape and color descriptors for all studied wheat lines.

DS	SKW	Area	PE	CI	FD	MFD	AR	RO	SO	H	S	I	L*	a*
Area	0.537 **													
PE	0.341	0.862 **												
CI	0.376 **	0.250	−0.269											
FD	0.192	0.696 **	0.960 **	−0.510 **										
MFD	0.583 **	0.793 **	0.401 **	0.743 **	0.152									
AR	−0.364 **	−0.180	0.320 *	−0.958 **	0.546 **	−0.734 **								
RO	0.306	0.106	−0.390 **	0.959 **	−0.610 **	0.674 **	−0.985 **							
SO	0.415 **	0.640 **	0.324 *	0.629 **	0.143	0.694 **	−0.459 **	0.437 **						
H	−0.300	−0.113	−0.161	0.016	−0.179	−0.134	0.085	−0.052	−0.015					
S	0.053	0.259	−0.030	0.475 **	−0.164	0.366 **	−0.354 **	0.342 *	0.464 **	0.679 **				
I	−0.094	−0.040	0.084	−0.234	0.151	−0.072	0.107	−0.121	−0.364 **	−0.225	−0.361 **			
L*	−0.147	0.080	−0.098	0.256	−0.176	0.118	−0.131	0.141	0.250	0.920 **	0.909 **	−0.328 *		
a*	0.356 **	0.158	0.169	0.047	0.166	0.197	−0.143	0.111	0.059	−0.989 **	−0.601 **	0.208	−0.879 **	
b*	0.016	0.228	−0.041	0.433 **	−0.165	0.318 *	−0.307 *	0.300 *	0.428 **	0.743 **	0.995 **	−0.367 **	0.944 **	−0.673 **

DS—descriptor, SKW—single kernel weight, PE—Perimeter, CI—Circularity, FD—Feret diameter, MFD—minimal Feret diameter, AR—Aspect ratio, RO—roundness, SO—solidity, H—hue, S—saturation, I—intensity, L*—luminance, a* indicates redness–greenness, and b* indicates yellowness–blueness. **— significant at $p \leq 0.01$, *—significant at $p \leq 0.05$.

3.5. Principal Component Analysis

PCA supported the very strong discrimination of all studied wheat taxa in terms of the combined effect of shape and color (Figure 5). A total of six clusters were identified, each containing elements characteristic of a given wheat species. The combined effect of PC1 and PC2 explained 65.6% of total variance. The correlation coefficients between the contribution of the variable (PC) to PC1 and PC2 are presented in Table 6. The perimeter had the weakest influence on discrimination, based on PC1, whereas FD, L^* , and S had the smallest effect on discrimination based on PC2. The combined contribution of PC1 and PC2 for eight shape descriptors was determined at 0.483 and 0.544, respectively, and for six color descriptors—at 0.516 and 0.457, respectively. The above indicates that shape and color variables had a similar influence. The principal component analysis validated the results of hierarchical clustering for shape and color components of kernel images. Wheat lines characterized by the lowest species diversity were grouped separately. Bread wheat lines formed separate clusters (Figures 2 and 3) and a separate group of objects (Figure 5). Similar observations were made in a durum wheat line. The strong discrimination of Polish wheat, which was grouped with spelt and emmer lines in cluster analysis, was confirmed by PCA (Figure 5).

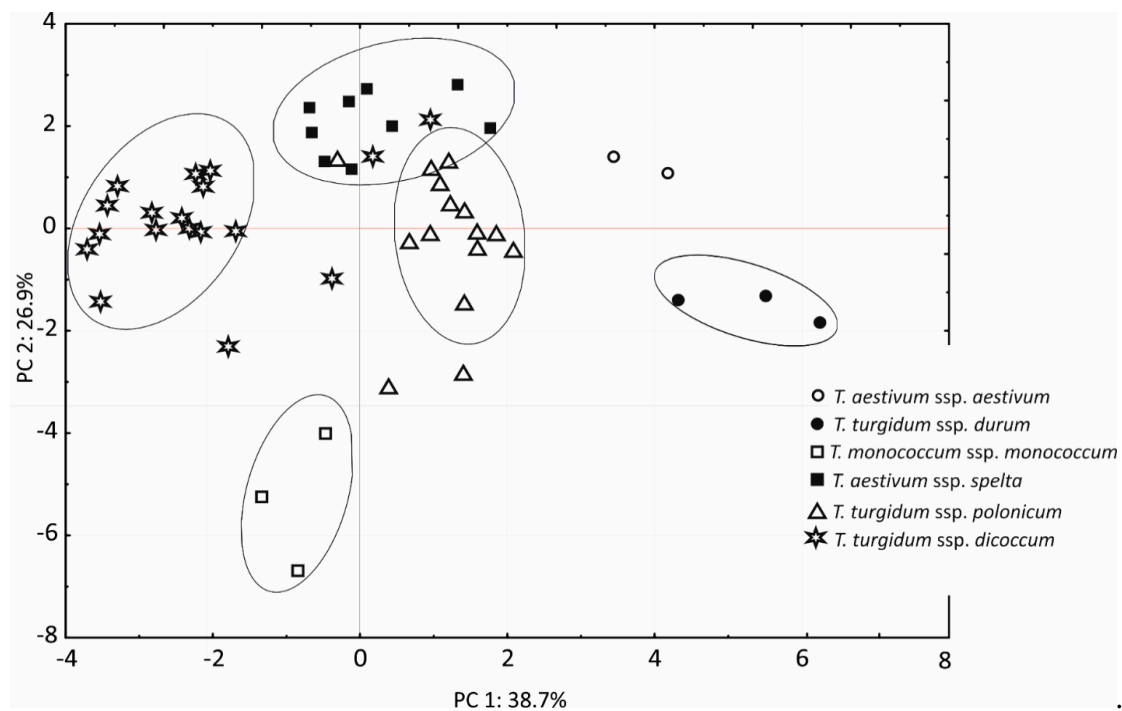


Figure 5. The results of principal component analysis (PCA) for shape and color descriptors of wheat species. Gaussian distribution confidence ellipses were drawn for the probability of 80%.

Table 6. Correlation coefficients (*r*) between a variable and a principal component (PC) and the contribution of each variable to the PCs.

Variable	<i>r</i>		Variable Contribution	
	PC 1	PC 2	PC 1	PC 2
Area	0.279 *	0.611 **	0.014	0.099
PE	−0.166	0.402 **	0.005	0.043
CI	0.805 **	0.457 **	0.120	0.056
FD	−0.378 **	0.252	0.026	0.017
MFD	0.603 **	0.731 **	0.067	0.142
AR	−0.703 **	−0.501 **	0.091	0.067
RO	0.702 **	0.449 **	0.091	0.053
SO	0.613 **	0.501 **	0.069	0.067
<i>H</i>	0.542 **	−0.760 **	0.054	0.153
<i>S</i>	0.877 **	−0.264	0.142	0.019
<i>I</i>	−0.408 **	0.122	0.031	0.004
<i>L</i> *	0.768 **	−0.567 **	0.109	0.085
<i>a</i> *	−0.472 **	0.790 **	0.041	0.166
<i>b</i> *	0.867 **	−0.335 *	0.139	0.030

SKW—single kernel weight, PE—Perimeter, CI—Circularity, FD—Feret diameter, MFD—minimal Feret diameter, AR—Aspect ratio, RO—roundness, SO—solidity, *H*—hue, *S*—saturation, *I*—intensity, *L**—luminance, *a** indicates redness–greenness, and *b** indicates yellowness–blueness. **—significant at $p \leq 0.01$, *—significant at $p \leq 0.05$.

4. Discussion

The main objective of this study was to discriminate wheat subspecies characterized by high genetic diversity. Wheat grain was evaluated by digital image analysis.

A cluster analyses revealed close links independently between the shape and color of bread wheat, durum wheat, and Polish wheat grain in the major clusters. Most importantly, bread wheat and durum wheat lines were very closely grouped in the morphological analysis, probably due to the low variation in their gene pools and the resulting morphological similarities. Based on the analyzed shape and color descriptors, Polish wheat lines were grouped with the above species in the major cluster; however, Polish wheat diverged from the remaining taxa to a certain extent. The above could be attributed to considerable intraspecific variations in Polish wheat, where the values of shape and color descriptors differed considerably. Despite the morphological similarities between emmer and spelt, the divergence between spelt and emmer increased in terms of grain shape. Spelt and emmer generally did not form groups, and they also formed highly divergent groups. The neighboring internal nodes containing spelt and emmer lines were grouped. It cannot be ruled out that the shape of spelt grain has been altered by multiple mutations and domestication, whereas its color remained similar to emmer. This regularity was observed even when differences in fungal colonization were taken into account. Fungal mycelia differ in color, and they can influence the color of the seed coat.

Diploid wheat species have smaller grain than tetraploid wheat [47]. This observation was confirmed in our study where diploid einkorn was characterized by the smallest kernel image area (12.90 mm²). Kernel image area was significantly larger in the tetraploid species of emmer, Polish wheat, and durum wheat (17.26, 19.68 and 19.55 mm², respectively). A similar trend was noted in kernel image PE, which was smaller in the diploid einkorn (17.52 mm) than in tetraploid species (18.81–19.93 mm). According to Matsuoka [48], during the domestication of diploid wheats, the initially strongly elongated grain was improved to produce larger and wider grain. Many authors have noted that tetraploid wheats have elongated and large kernels [49–51]. Gegas et al. [52] emphasized that in the process of breeding high-yielding wheat cultivars, efforts are also made to obtain wheat with the plumpest grain. The large kernel image area and PE of the evaluated durum wheat lines point to selection for larger grain. Bread wheat was characterized by small grain, probably because long-term selection for grain with improved chemical composition and processing suitability has led to a reduction in grain size. Some genes encoding grain size could have also been

lost during selection. In breeding practice, the morphological traits of grain are evaluated for milling performance (flour quality). Bread wheat grain is processed into flour for baking and confectionery goods, whereas durum wheat is used in the production of semolina, groats, and couscous.

The evaluated lines of Polish wheat were characterized by high RSD values of most shape and color descriptors. High intraspecies variation can be attributed to the low commercial interest in this species; therefore, conscious efforts to narrow down the gene pool of Polish wheat were not made throughout the centuries [53]. A comparison of the variations in the lines of the analyzed wheat species suggests that rarely farmed ancient species are characterized by a larger gene pool and consequently, greater variations in phenotypic traits [54]. The results of our study indicate that the grain of bread wheat, and durum wheat had a regular structure, bread wheat grain was round, whereas durum wheat grain was elongated. The grain of ancient species had irregular shape, which can probably be attributed to the absence of prior selection for processing suitability. As mentioned earlier, einkorn was the only species that was not related to the remaining taxa. A comparison of shape descriptors indicates that einkorn grain differed noticeably from the remaining wheats—it was smaller, more elongated, and the least regular in shape. The closely related tetraploid species were most similar in PE, whereas the values of the remaining shape descriptors supported discrimination. The grain of the tetraploid durum wheat and the relatively closely related spelt were somewhat similar, mostly in terms of area, PE, MFD, AR, and RO. Phenotypic similarities could be attributed to gene flow from the parent species (durum wheat) to the progeny (spelt). A comparison of spelt and bread wheat, which evolved by the way of numerous mutations in *T. aestivum* ssp. *spelta*, reveals clear differences in grain shape. According to some mathematical models, milling yield could be increased by optimizing the shape and size of grain. Large and spherical grains are optimal [55], and these morphological traits are characteristic of bread wheat. Shape descriptors provide breeders information about kernels size (Area, PE), shape (i.e., high values of AR and FD or low values of RO point to elongated shape) and other features (SO describes shape regularity). The low values of correlation coefficients between grain image descriptors indicate that these components can be manipulated independently. In some cases, phenotyping could be less expensive than genetic analysis, especially when a single stable trait is analyzed. However, the phenotyping of large populations is still expensive in field trials where several traits are evaluated. The dynamic nature of many plants traits requires multiple measurements during plant development. Variation in plants can be accurately determined based on genotypic information that is associated only with phenotypic data. Digital image analysis is considered a high-throughput method, due to the low cost of the sensor (i.e., scanner or digital camera), access to free software for image processing, and advanced solutions that support simultaneous analyses of large datasets [56]. Digital image analysis is also well suited for pre-selection [57]. Its usefulness has been demonstrated by numerous studies [28,57–61].

Another objective of this study was to determine whether grain colonization by endophytic fungal pathogens influences the values of color descriptors of kernel images. The images of bread wheat kernels were characterized by average values of lightness and saturation, whereas spelt and emmer grain was more red, which could be partially attributed to colonization by *F. poae*. In studies by Suchowilska et al. [62] and Oliver et al. [63], selected emmer lines exhibited partial or moderate resistance to FHB. For this reason, fungal grain colonization and the prevalence of fungal infections should be closely monitored to identify supportive conditions for the growth of *Fusarium* spp. and other mycotoxin-producing fungi. Kernel color is also determined by reddish phenolic compounds, such as anthocyanins and flavonoids [64], and pericarp structure [65]. Durum wheat grain is characterized by light color and a yellow-reddish hue, which points to a different composition of phenolic compounds and different pericarp structure than spelt and emmer. However, the absence of significant correlations between fungal colonization and the color of the seed coat suggests that fungi had a minor influence on the discrimination of the evaluated genotypes. This implies that discrimination is conditioned mainly by the plant's genotype.

Principal component analysis strongly discriminated three species: bread wheat, durum wheat, and einkorn. In the remaining wheat species, individual lines were grouped with other taxa, which could be due to similarities in the degree of ploidy (Polish wheat and emmer), as well as significant intraspecific variations in Polish wheat, which could explain the grouping of one Polish wheat line with spelt. However, it should be noted that most Polish wheat lines were positioned in the middle range of the values noted in the remaining species.

The grains of wheats other than *T. aestivum* ssp. *aestivum* and *T. turgidum* ssp. *durum* is expensive. The addition of durum wheat or bread wheat flour to whole grain flour can effectively lower the price of the final product. Durum wheat and bread wheat are abundant in gluten, a potent allergen; therefore, the quantity and source of grain in the end product should be identified and presented on the label. According to Lombardo et al. [2], einkorn gluten is less immunoreactive, and it could be a potential candidate in the production of hypoallergenic bakery goods. Only certified grain and seeds should be traded on the cereal market. Methods that support quick identification of grain batches and admixtures of other cereal species not only protect agricultural producers, but also prevent consumers from purchasing products that do not meet their expectations.

In this study, attempts were made to validate the existing image processing methods by evaluating specific plant material, namely the grain of ancient wheats characterized by high genetic and phenotypic variation. The results of this experiment indicate that digital image analysis is an effective method of discriminating wheat species with high genetic variation. Shape and color descriptors were strongly discriminating components in studied wheat species. Their discriminatory power was determined mainly by genotype. Ancient diploid, tetraploid, and hexaploid wheats were subjected to image processing for the first time. Digital image analysis supported the extraction of multiple features, and it is a valuable tool for examining grain quality [56].

Author Contributions: Conceptualization, M.W.; Methodology, M.W.; Software, M.W.; Validation, K.G.-D., A.D., U.W., M.W.; Formal Analysis, K.G.-D. and A.D.; Investigation, K.G.-D. and A.D.; Resources, M.W.; Data Curation, K.G.-D.; Writing—Original Draft Preparation, K.G.-D.; Writing—Review & Editing, K.G.-D. and A.D.; Visualization, K.G.-D., A.D. and M.W.; Supervision, M.W.; Project Administration, M.W.; Funding Acquisition, M.W.

Funding: This research received no external funding.

Conflicts of Interest: The authors declare no conflict of interest.

References

1. Maccaferri, M.; Mantovani, P.; Tuberosa, R.; DeAmbrogio, E.; Giuliani Demontis, A.; Massi, A.; Sanguineti, M.C. A major QTL for durable leaf rust resistance widely exploited in durum wheat breeding programs maps on the distal region of chromosome arm 7BL. *Theor. Appl. Genet.* **2008**, *117*, 1225–1240. [[CrossRef](#)] [[PubMed](#)]
2. Lombardo, C.; Bolla, M.; Chignola, R.; Senna, G.; Rossin, G.; Caruso, B.; Tomelleri, C.; Cecconi, D.; Brandolini, A.; Zoccatelli, G. Study on the immunoreactivity of *Triticum monococcum* (Einkorn) wheat in patients with wheat-dependent exercise-induced anaphylaxis for the production of hypoallergenic foods. *J. Agric. Food Chem.* **2015**, *63*, 8299–8306. [[CrossRef](#)] [[PubMed](#)]
3. Henkrar, F.; El-Haddoury, J.; Ouabbou, H.; Nsarellah, N.; Iraqi, D.; Bendaou, N.; Udupa, S.M. Genetic diversity and its temporal changes in improved bread wheat cultivars of Morocco. *Rom. Agric. Res.* **2015**, *32*, 19–25.
4. Moragues, M.; Moralejo, M.; Sorrells, M.E.; Royo, C. Dispersal of durum wheat [*Triticum turgidum* L. ssp. *turgidum* convar. *durum* (Desf.) MacKey] landraces across the Mediterranean basin assessed by AFLPs and microsatellites. *Genet. Resour. Crop Evol.* **2007**, *54*, 1133–1144. [[CrossRef](#)]
5. Figliuolo, G.; Perrino, P. Genetic diversity and intra-specific phylogeny of *Triticum turgidum* L. subsp. *dicoccon* (Schrank) Thell. revealed by RFLPs and SSRs. *Genet. Resour. Crop Evol.* **2004**, *51*, 519–527. [[CrossRef](#)]
6. Jing, H.C.; Bayon, C.; Kanyuka, K.; Berry, S.; Wenzl, P.; Huttner, E.; Kilia, A.; Hammond-Kosack, K.E. DArT markers: Diversity analyses, genomes comparison, mapping and integration with SSR markers in *Triticum monococcum*. *BMC Genom.* **2009**, *10*, 458. [[CrossRef](#)] [[PubMed](#)]

7. Fernandez, M.R.; Sissons, M.; Conner, R.L.; Wang, H.; Clarke, J.M. Influence of biotic and abiotic factors on dark discoloration of durum wheat kernels. *Crop Sci.* **2011**, *51*, 1205–1214. [[CrossRef](#)]
8. Wang, H.; Fernandez, M.R.; McCaig, T.N.; Gan, Y.T.; DePauw, R.M.; Clarke, J.M. Kernel discoloration and downgrading in spring wheat varieties in western Canada. *Can. J. Plant Pathol.* **2003**, *25*, 350–361. [[CrossRef](#)]
9. Fares, C.; Codianni, P.; Nigro, F.; Platani, C.; Scazzina, F.; Pellegrini, N. Processing and cooking effects on chemical, nutritional and functional properties of pasta obtained from selected emmer genotypes. *J. Sci. Food. Agric.* **2008**, *88*, 2435–2444. [[CrossRef](#)]
10. Hidalgo, A.; Brandolini, A.; Gazza, L. Influence of steaming treatment on chemical and technological characteristics of einkorn (*Triticum monococcum* L. ssp. *monococcum*) wholemeal flour. *Food Chem.* **2008**, *111*, 549–555. [[CrossRef](#)]
11. Kucek, L.K.; Dyck, E.; Russell, J.; Clark, L.; Hamelman, J.; Burns-Leader, S.; Senders, S.; Jones, J.; Benschler, D.; Davis, M.; et al. Evaluation of wheat and emmer varieties for artisanal baking, pasta making, and sensory quality. *J. Cereal Sci.* **2017**, *74*, 19–27. [[CrossRef](#)]
12. European Commission. Commission Regulation (EC) No 2073/2005 on microbiological criteria for foodstuffs. *Off. J. Eur. Union* **2005**, *50*, 1–26.
13. Khatri, Y.; Collins, R. Impact and status of HACCP in the Australian meat industry. *Br. Food J.* **2007**, *109*, 343–354. [[CrossRef](#)]
14. Narendra, V.G.; Hareesh, K. Prospects of computer vision automated grading and sorting systems in agricultural and food products for quality evaluation. *Int. J. Comput. Appl.* **2010**, *1*, 651–657. [[CrossRef](#)]
15. CBH Group. 2018. Available online: <https://cbh.com.au/other%20information/quality%20services/eyefoss> (accessed on 1 July 2018).
16. Sun, Q.; Wu, L.; Ni, Z.; Meng, F.; Wang, Z.; Lin, Z. Differential gene expression patterns in leaves between hybrids and their parental inbreds are correlated with heterosis in a wheat diallel cross. *Plant Sci.* **2004**, *166*, 651–657. [[CrossRef](#)]
17. Scanalyzer HTS: LemnaTec GmbH, Germany. 2018. Available online: <https://www.lemnatec.com/products/laboratory/lab-scanalyzer-hts/> (accessed on 1 July 2018).
18. Neuman, M.; Sapirstein, H.D.; Shwedyk, E.; Bushuk, W. Discrimination of wheat class and variety by digital image analysis of whole grain samples. *J. Cereal Sci.* **1987**, *6*, 125–132. [[CrossRef](#)]
19. Neuman, M.R.; Sapirstein, H.D.; Shwedyk, E.; Bushuk, W. Wheat grain colour analysis by digital image processing II. Wheat class discrimination. *J. Cereal Sci.* **1989**, *10*, 183–188. [[CrossRef](#)]
20. Zayas, I.; Pomeranz, Y.; Lai, F.S. Discrimination of wheat and nonwheat components in grain samples by image analysis. *Cereal Chem.* **1989**, *66*, 233–237.
21. Mirik, M.; Michels, G.J., Jr.; Kassymzhanova-Mirik, S.; Elliott, N.C.; Catana, V.; Jones, D.B.; Bowling, R. Using digital image analysis and spectral reflectance data to quantify damage by greenbug (*Hemiteara: Aphididae*) in winter wheat. *Comput. Electron. Agric.* **2006**, *51*, 86–98. [[CrossRef](#)]
22. Yan, X.; Wang, J.; Liu, S.; Zhang, C. Purity Identification of Maize Seed Based on Color Characteristics. In *Computer and Computing Technologies in Agriculture IV, Proceedings of the International Conference on Computer and Computing Technologies in Agriculture, Nanchang, China, 22–25 October 2010*; Li, D., Liu, Y., Chen, Y., Eds.; Springer: Berlin/Heidelberg, Germany, 2011; Volume 346, ISBN 978-3-642-18354-6.
23. Diéguez-Urbeondo, J.; Förster, H.; Adaskaveg, J.E. Digital image analysis of internal light spots of appressoria of *Colletotrichum acutatum*. *Phytopathology* **2003**, *93*, 923–930. [[CrossRef](#)]
24. Wijekoon, C.P.; Goodwin, P.H.; Hsiang, T. Quantifying fungal infection of plant leaves by digital image analysis using Scion Image software. *J. Microbiol. Meth.* **2008**, *74*, 94–101. [[CrossRef](#)] [[PubMed](#)]
25. Suchowilska, E.; Wiwart, M. Multivariate analysis of image descriptors of common wheat (*Triticum aestivum*) and spelt (*T. spelta*) grain infected by *Fusarium culmorum*. *Int. Agrophys.* **2006**, *20*, 345.
26. Bauriegel, E.; Giebel, A.; Geyer, M.; Schmidt, U.; Herppich, W.B. Early detection of *Fusarium* infection in wheat using hyper-spectral imaging. *Comput. Electron. Agric.* **2011**, *75*, 304–312. [[CrossRef](#)]
27. Ahmad, I.S.; Reid, J.F.; Paulsen, M.R.; Sinclair, J.B. Color classifier for symptomatic soybean seeds using image processing. *Plant Dis.* **1999**, *83*, 320–327. [[CrossRef](#)]
28. Leplat, J.; Mangin, P.; Falchetto, L.; Heraud, C.; Gautheron, E.; Steinberg, C. Visual assessment and computer-assisted image analysis of *Fusarium* head blight in the field to predict mycotoxin accumulation in wheat grains. *Eur. J. Plant Pathol.* **2018**, *150*, 1065–1081. [[CrossRef](#)]

29. Zapotoczny, P. Discrimination of wheat grain varieties using image analysis and neural networks. Part I. Single kernel texture. *J. Cereal Sci.* **2011**, *54*, 60–68. [[CrossRef](#)]
30. Wiwart, M.; Suchowilska, E.; Lajszner, W.; Graban, L. Identification of hybrids of spelt and wheat and their parental forms using shape and color descriptors. *Comput. Electron. Agric.* **2012**, *83*, 68–76. [[CrossRef](#)]
31. Zielinska, M.; Zapotoczny, P.; Białobrzewski, I.; Zuk-Gołaszewska, K.; Markowski, M. Engineering properties of red clover (*Trifolium pratense* L.) seeds. *Ind. Crop. Prod.* **2012**, *37*, 69–75. [[CrossRef](#)]
32. Ropelewska, E.; Zapotoczny, P.; Budzyński, W.S.; Jankowski, K.J. Discriminating power of selected physical properties of seeds of various rapeseed (*Brassica napus* L.) cultivars. *J. Cereal Sci.* **2017**, *73*, 62–67. [[CrossRef](#)]
33. Chaugule, A.A.; Mali, S.N. Identification of paddy varieties based on novel seed angle features. *Comput. Electron. Agric.* **2016**, *123*, 415–422. [[CrossRef](#)]
34. Cervantes, E.; Martín, J.J.; Saadaoui, E. Updated Methods for Seed Shape Analysis. *Scientifica* **2016**. [[CrossRef](#)] [[PubMed](#)]
35. Sun, Y. Hopfield neural network based algorithms for image restoration and reconstruction. I. Algorithms and simulations. *IEEE Trans. Signal Process.* **2000**, *48*, 2105–2118. [[CrossRef](#)]
36. Russ, J.C. Segmentation and thresholding. In *The Image Processing Handbook*, 6th ed.; CRC, Taylor & Francis Group: New York, NY, USA, 2016; pp. 395–443, ISBN 9781439840634.
37. Szczypiński, P.M.; Klepaczko, A.; Kociólek, M. QMaZda—Software tools for image analysis and pattern recognition. In Proceedings of the 2017 Signal Processing: Algorithms, Architectures, Arrangements, and Applications (SPA), Poznan, Poland, 20–22 October 2017; pp. 217–221.
38. Bock, C.H.; Poole, G.H.; Parker, P.E.; Gottwald, T.R. Plant Disease Severity Estimated Visually, by Digital Photography and Image Analysis, and by Hyperspectral Imaging. *Crit. Rev. Plant Sci.* **2010**, *29*, 59–107. [[CrossRef](#)]
39. Cope, P. *The Digital Photographer's Pocket Encyclopedia: 3000 Terms Explained*; Silver Pixel Press: Rochester, NY, USA, 2002; ISBN 1883403901.
40. Steddom, K.; Bredehoeft, M.W.; Khan, M.; Rush, C.M. Comparison of visual and multispectral radiometric disease evaluations of Cercospora leaf spot of sugar beet. *Plant Dis.* **2005**, *89*, 153–158. [[CrossRef](#)]
41. Rasband, W.S. *ImageJ*; U.S. National Institutes of Health: Bethesda, MD, USA, 2016. Available online: <https://imagej.nih.gov/ij/> (accessed on 1 July 2018).
42. Wiwart, M.; Fordoński, G.; Żuk-Gołaszewska, K.; Suchowilska, E. Early diagnostics of macronutrient deficiencies in three legume species by color image analysis. *Comput. Electron. Agric.* **2009**, *65*, 125–132. [[CrossRef](#)]
43. Follstad, M.N.; Christensen, C.M. Microflora of barley kernels. *Appl. Microbiol.* **1962**, *10*, 331–336. [[PubMed](#)]
44. Ellis, M.B.; Ellis, J.P. (Eds.) *Microfungi on Land Plants: An Identification Handbook*; Richmond Publishing: Slough, UK, 1987.
45. Leslie, J.F.; Summerell, B.A. (Eds.) *The Fusarium Laboratory Manual*; Wiley-Blackwell Publishing: Ames, IA, USA, 2006.
46. StatSoft. *STATISTICA (Data Analysis Software System)*; Version 12; StatSoft, Inc.: Tulsa, OK, USA, 2014; Available online: www.statsoft.com (accessed on 1 July 2018).
47. Fuller, D.Q. Contrasting patterns in crop domestication and domestication rates: Recent archaeobotanical insights from the Old World. *Ann. Bot.* **2007**, *100*, 903–924. [[CrossRef](#)] [[PubMed](#)]
48. Matsuoka, Y. Evolution of polyploid *Triticum* wheats under cultivation: The role of domestication, natural hybridization and allopolyploid speciation in their diversification. *Plant Cell Physiol.* **2011**, *52*, 750–764. [[CrossRef](#)] [[PubMed](#)]
49. Bakhteyev, F.K.; Yanushevich, Z.V. Discoveries of cultivated plants in the early farming settlements of Yarym-Tepe I and Yarym-Tepe II in northern Iraq. *J. Archaeol. Sci.* **1980**, *7*, 167–178. [[CrossRef](#)]
50. Jacomet, S. Identification of Cereal Remains from Archaeological Sites. 2006. Available online: <http://arkeobotanika.pbworks.com/f/Jacomet+cereal+ID.pdf> (accessed on 1 July 2018).
51. Okamoto, Y.; Takumi, S. Pleiotropic effects of the elongated glume gene P1 on grain and spikelet shape-related traits in tetraploid wheat. *Euphytica* **2013**, *194*, 207–218. [[CrossRef](#)]
52. Gegas, V.C.; Nazari, A.; Griffiths, S.; Simmonds, J.; Fish, L.; Orford, S.; Sayers, L.; Doonan, J.H.; Snape, J.W. A genetic framework for grain size and shape variation in wheat. *Plant Cell* **2010**, *22*, 1046–1056. [[CrossRef](#)] [[PubMed](#)]

53. Eticha, F.; Belay, G.; Bekele, E. Species diversity in wheat landrace populations from two regions of Ethiopia. *Genet. Resour. Crop. Evol.* **2006**, *53*, 387–393. [[CrossRef](#)]
54. Cifci, E.A.; Yagdi, K. Study of genetic diversity in wheat (*Triticum aestivum*) varieties using random amplified polymorphic DNA (RAPD) analysis. *Turk. J. Field Crops* **2012**, *17*, 91–95.
55. Evers, A.D.; Cox, R.I.; Shaheedullah, M.Z.; Withey, R.P. Predicting milling extraction rate by image analysis of wheat grains. *Asp. Appl. Biol.* **1990**, *25*, 417–426.
56. Zhang, C.; Si, Y.; Lamkey, J.; Boydston, R.A.; Garland-Campbell, K.A.; Sankaran, S. High-Throughput Phenotyping of Seed/Seedling Evaluation Using Digital Image Analysis. *Agronomy* **2018**, *8*, 63. [[CrossRef](#)]
57. Williams, K.; Munkvold, J.; Sorrells, M. Comparison of digital image analysis using elliptic Fourier descriptors and major dimensions to phenotype seed shape in hexaploid wheat (*Triticum aestivum* L.). *Euphytica* **2013**, *190*, 99–116. [[CrossRef](#)]
58. Breseghello, F.; Sorrells, M.E. Association mapping of kernel size and milling quality in wheat (*Triticum aestivum* L.) cultivars. *Genetics* **2006**, *172*, 1165–1177. [[CrossRef](#)]
59. Breseghello, F.; Sorrells, M.E. QTL analysis of kernel size and shape in two hexaploid wheat mapping populations. *Field Crops Res.* **2007**, *101*, 172–179. [[CrossRef](#)]
60. Dana, W.; Ivo, W. Computer image analysis of seed shape and seed color for flax cultivar description. *Comput. Electron. Agric.* **2008**, *61*, 126–135. [[CrossRef](#)]
61. Jamil, M.; Ali, A.; Ghafoor, A.; Akbar, K.F.; Napar, A.A.; Naveed, N.H.; Yasin, N.A.; Gul, A.; Mujeeb-Kazi, A. Digital image analysis of seed shape influenced by heat stress in diverse bread wheat germplasm. *Pak. J. Bot.* **2017**, *49*, 1279–1284.
62. Suchowilska, E.; Kandler, W.; Sulyok, M.; Wiwart, M.; Krska, R. Mycotoxin profiles in the grain of *Triticum monococcum*, *Triticum dicoccum* and *Triticum spelta* after head infection with *Fusarium culmorum*. *J. Sci. Food Agric.* **2010**, *90*, 556–565. [[PubMed](#)]
63. Oliver, R.E.; Cai, X.; Friesen, T.L.; Halley, S.; Stack, R.W.; Xu, S.S. Evaluation of Fusarium head blight resistance in tetraploid wheat (*Triticum turgidum* L.). *Crops Sci.* **2008**, *48*, 213–222. [[CrossRef](#)]
64. Shen, Y.; Jin, L.; Xiao, P.; Lu, Y.; Bao, J. Total phenolics, flavonoids, antioxidant capacity in rice grain and their relations to grain color, size and weight. *J. Cereal Sci.* **2009**, *49*, 106–111. [[CrossRef](#)]
65. Burešová, V.; Kopecký, D.; Bartoš, J.; Martinek, P.; Watanabe, N.; Vyhnánek, T.; Doležel, J. Variation in genome composition of blue-aleurone wheat. *Theor. Appl. Genet.* **2015**, *128*, 273–282. [[CrossRef](#)]



© 2018 by the authors. Licensee MDPI, Basel, Switzerland. This article is an open access article distributed under the terms and conditions of the Creative Commons Attribution (CC BY) license (<http://creativecommons.org/licenses/by/4.0/>).